**Original Article****Effects of ultrasound time on the properties of polyvinyl alcohol-based nanocomposite films**Akbar Jokar<sup>1</sup>, Mohamad Hossein Azizi<sup>2\*</sup>, Zohre Hamidi Esfehani<sup>2</sup>

1- Ph.D. Student, Dept. of Food Science, College of Agriculture, Tarbiat Modares University, Tehran, Iran.

2- Dept. of Food Science, College of Agriculture, Tarbiat Modares University, Tehran, Iran

**Received:** May 2015**Accepted:** August 2015**ABSTRACT**

**Background and Objectives:** Preparation and evaluation of nanocomposite films have become prevalent in recent years. One of the most important methods for dispersing nanoparticles in polymers is the use of ultrasound radiation. Polyvinyl alcohol-montmorillonite (PVA-MMT) nanocomposite films were prepared via solvent casting method.

**Materials and Methods:** The effects of different ultrasound times (0, 10, 20, 30, and 40 min) on the properties of nanocomposite films were evaluated in a completely randomized design (CRD) with five treatments and three replicates. The films were characterized by mechanical properties, opacity, water vapor permeability (WVP), and color. Fourier transform infrared (FTIR) and X-ray diffraction (XRD) were applied to investigate and prove the effects of ultrasound time.

**Results:** Results revealed that the ultrasound time significantly affected the characteristics of the films. XRD and FTIR results were in accordance with the effects of sonication time. The changing trends of PVA film properties due to increasing the sonication times were not similar. Sonication time did not have any significant effect on some traits like  $a^*$ , WVP,  $L^*$ , and yellowness index (YI), while it affected  $b^*$ , tensile strength, and opacity significantly.

**Conclusions:** Depending on the target of using nanocomposite films, appropriate time of sonication should be used.

**Keywords:** Ultrasound time, Polyvinyl alcohol, Nanocomposite film, Nanoclay, FTIR, X-ray

**Introduction**

Since 1970, the production and use of plastics in the world have been extensively increased. Waste disposal problems have pushed studies toward the development of polymers that could be degraded more rapidly in the environment (mineralization or bioassimilation). Designing, synthesizing, and using biodegradable polymers, especially natural ones, offer a possible alternative to these non-biodegradable materials, in particular when their collection and processing are not possible and economical (1, 2). The most important barriers in applying biodegradable natural materials, especially for packaging, are their poor mechanical, thermal, and moisture resistance properties. Recently,

nanocomposites such as polymer-layered silicate have become prevalent. Silicate layers should have at least one dimension of less than 100 nm (3-5). MMT is a type of silicate clay that has been widely used in polymer nanocomposites. High intercalation chemistry, strength, abundance in nature, low gas permeability, safety, and economic properties of MMT have led to the widespread use of this material (6-9).

Many investigations have shown that incorporating nano-scaled silicate layers into polymers increases their mechanical properties, heat, and moisture resistance, and also decreases their moisture adsorption, permeability, and flammability (8, 10).

\*Address for correspondence: Mohamad Hossein Azizi, Associate prof, Dept. of Food Science, College of Agriculture, Tarbiat Modares University, Tehran, Iran, E-mail address: aziz\_m@modares.ac.ir.

Depending on silicate dispersion, two types of nanocomposite, i.e. intercalated and exfoliated, can be obtained. The latter is known as *delaminated silicate*, and is preferred to the former because of having better barrier and mechanical properties (3, 8, 9, 11, 12).

Producing clay nanocomposites can be usually achieved by 3 methods: *in situ* polymerization, melt compounding, and solvent blending/casting. Researchers have applied suitable blending methods such as shear, high pressure, centrifuge, and ultrasonication mixing for producing a high performance nanocomposite. Ultrasonication is one of the most important methods for increasing intergallery spacing between silicate layers and dispersing them in the polymers. Ultrasound treatment can help in terms of easily achieving exfoliated clay structure and increasing d-spacing in comparison to non-sonicated samples (13). Furthermore, ultrasonication widely affects the polymer itself and, as a result, changes nanocomposites' properties. So, power and time of sonication are critical, and should be seriously considered in nanocomposite preparations (3, 14-17). Ultrasound treatment induces physical and chemical changes in the substances, which are exposed to ultrasound radiation. Acoustic cavitations, bubbles, and their collapses are the main reasons for these changes. Bubble violent explosion generates extreme temperature and pressure inside the bubbles and solvent. So, the materials in the solvent are disintegrated and several highly reactive radicals would be generated. Several chemical reactions can occur between these active radicals and substances in the medium. Finally, more chemical bonds like H and covalent bonds will be generated (16, 18).

Alshabanat et al. found that increasing the sonication time in polystyrene resulted in the creation of crystalline structures in the amorphous region. The maximum peak intensity in the XRD was obtained after 1h of sonicating polystyrene- MMT nanocomposite, which showed higher interaction and chemical bonds with MMT (3). Intergallery spacing of epoxy-clay nanocomposite increased with increasing the sonication time at low clay loading (2%). Dispersion of nanoclay at high sonication times was significantly better. Increase of sonication time enhanced tensile strength, while hardness did not change (15). Chen et al. revealed that 15 min ultrasound time could break cross-links between

amylose and amylopectin in maze starch, which in turn caused depletion in opacity, WVP, elongation in the films, and increased tensile strength (16). Ultrasound and microwave combination, especially lower than 20 min, can significantly affect barrier and mechanical properties of nanocomposite films from methyl cellulose, wheat bran cellulose, and soy protein (17, 19-21). To the best our knowledge, there are a few reports proving the effects of ultrasound time on preparing popular nanocomposite films like PVA (22, 23).

PVA is a safe and synthetic polymer, which is used widely in industrial, commercial, medical and food applications (24). There are lots of developments in PVA-based nanocomposite films and its blend with starch and other biodegradable polymers. PVA can be employed in food packaging as it shows a broad and universe range of suitable technological properties, as well as user friendly characteristics like low cost and approximate high biodegradation rate (25, 26).

The present research was designed to show and prove the relationship between sonication time and properties of PVA-MMT nanocomposite films, and to illustrate how sonication time will affect nanocomposites' properties. The research was also designed to show the importance of sonication time optimization.

## Materials and Methods

**Materials:** PVA was supplied from LOBA Chemie, Mumbai, India (Polymerization degree: 1700-1800, Viscosity of its 2% solution 25-32 cp, Hydrolysis: 98-99% mole). MMT without any modifications was supplied from Southern Clay Products Inc., USA (Cloisite Na<sup>+</sup>). Glycerol (Pub Chem CID: 753) was purchased from the Merck Company, Germany.

**MMT characterizations:** Particle size distribution of MMT suspensions was assessed using Malvern Zetasizer, Nanoseries, Nano-ZS (UK). Samples of MMT suspension were collected just before adding it to the polymer solution (Fig.1) and then diluted to proper concentration for analysis by Zetasizer. XRD measurement (XPertMPD, Philips, Holland XRD) showed the initial space between the silicate layers.

**MMT preparation:** MMT preparation is illustrated in Fig. 1. All of the nanoclay preparations were carried out in 100 ml laboratory beakers. Stirrers and magnet stirring sets were Heidolf MR 3001 (Germany) and 2 cm magnet, respectively. In nanoclay preparations, a water bath sonicator was

used (ULTRASONS-H, PSelecta CE95, 50 kHz, 1000W). At all stages of nanoclay preparation, the top of the beakers was wrapped tightly with a soft polyethylene sheet to avoid water vaporization.

**Film preparation:** Each polymer has individual characteristics and the method of film preparation is exclusive. The process of film preparation is illustrated in Fig. 2. In the nanocomposite preparation, stirrer and magnet stirring were Heidolf MR 3001 and 6 cm magnet, respectively. In nanocomposite preparation, a water bath sonicator was used (ULTRASONS-H, PSelecta CE95, 50 kHz, 1000W). From the beginning to the end of nanocomposite preparation, 500 ml blue cap glass containers were used and tightly capped to avoid the solvent evaporation.

**Properties of PVA nanocomposite films:** The nanocomposite films were characterized by mechanical properties (tensile strength and elongation at break), opacity, WVP, color, YI, and thickness. XRD was used to investigate the dispersion of MMT

in PVA polymer. FTIR spectroscopy was applied to show chemical bonds and the interaction between MMT and PVA/glycerol at different sonication times.

**Mechanical properties:** Tensile strength and elongation at break evaluations were performed using a texture analyzer (Instron, Hounsfield H50KS, England) according to ASTM D882-12 (27). Speed of upper Instron's jaw was 50 mm/min. Rectangular strips (8\*1 cm) were cut from the film sheets, and 2 cm from the top and bottom of the strips was carefully wrapped using adhesive paper scotch. The latter was done to avoid compression, rupture, and slipping of the films between the Instron's jaws. The distance between the jaws was 4 cm. The strips were equilibrated at 25 °C and 50% RH for 72 h before doing the test.

Initial Young's modulus or modulus of elasticity was calculated from the slope of the initial linear region of the stress-strain curve at very small strain or elongation at break (28).

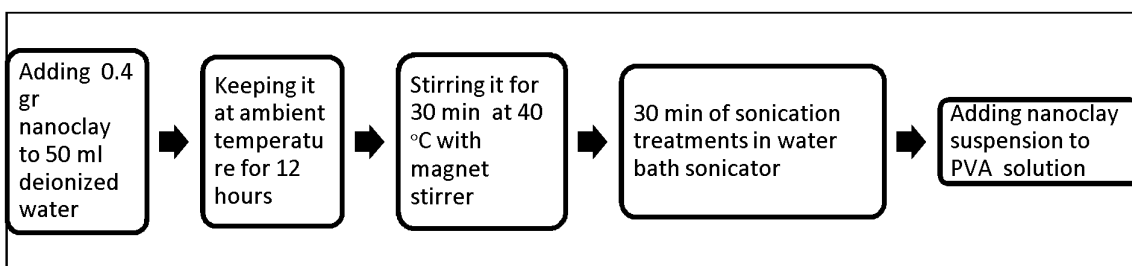


Figure 1. Nanoclay preparation

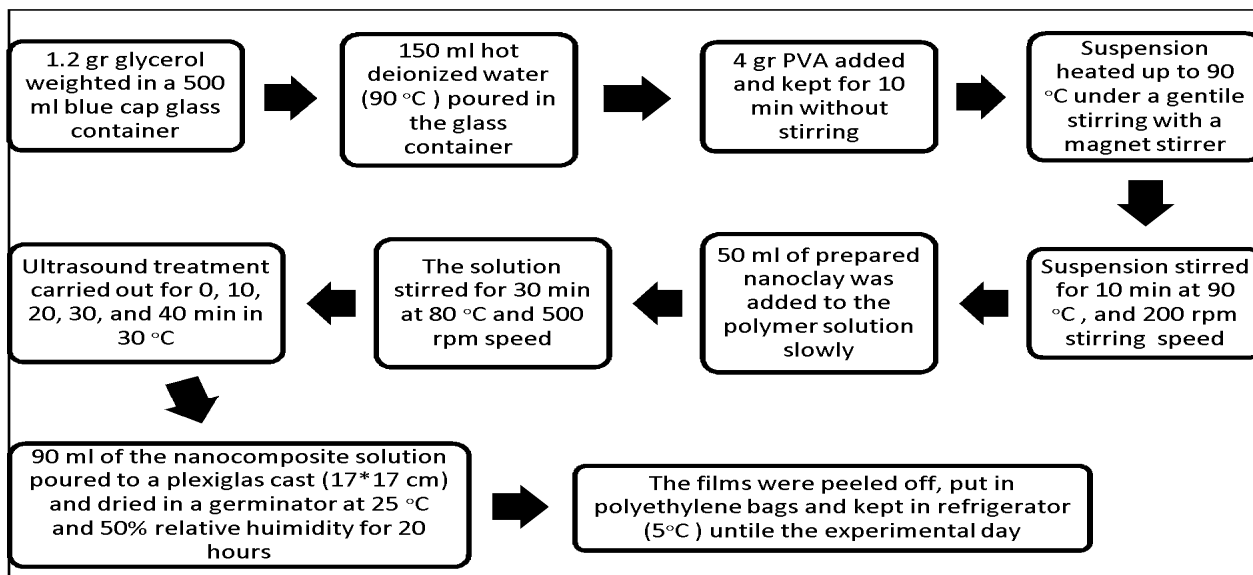


Figure 2. Preparation of PVA nanocomposite films

**X-ray diffraction (XRD):** Exfoliate and intercalate structures of PVA nanocomposite films were evaluated using X'PertMPD, Philips, Holland XRD, diffractometer equipped with CO K $\alpha$  1.79  $\text{\AA}$  (scanning rate of 0.02°/S, scan step time of 2s, voltage of 40 kv, and current of 30 mA). Data collection was done at 2 $\theta$  angle from 1 to 12°.

The XRD software calculated the d-spacing of MMT layers based on Bragg equation (29):

$$\lambda = 2d\sin\theta \quad (\text{Eq. 1})$$

Where,  $\lambda$  is wavelength of the X-ray beam (nm),  $d$  is spacing (nm) between the two layers, and  $\theta$  is the angle of incidence.

**Fourier transform infrared spectroscopy (FTIR):** FTIR spectra were collected using FTIR spectrometer (Nexus 6700, Thermo Nicolet, USA). Transmission method was applied to the nanocomposite films. IR absorption spectra of the nanocomposite films were obtained for the purposes of measuring and scanning. The spectral collections were performed in the wavenumber range of 400–4000  $\text{cm}^{-1}$  with the resolution of 4  $\text{cm}^{-1}$ .

**Opacity:** Opacity of the nanocomposite films was measured using a Cary 60 UV/VIS spectrophotometer (USA). Rectangular pieces of the films were prepared and put in the sample position of the spectrophotometer. Empty measurement was used as the reference. The opacity of the films was calculated as below (8, 30, 31):

$$\text{Opacity} = \frac{\text{Abs}600}{X} \quad (\text{Eq. 2})$$

Where,  $\text{Abs}600$  is absorbance at 600 nm, and  $X$  is the thickness (mm) of the films.

**Water Vapor Permeability (WVP):** The WVP evaluations were based on the modified ASTM E96/E96 M-14 method (32). Before running the test, the circle samples ( $19.625 \times 10^{-4} \text{ m}^2$  in the surface area) were cut and equilibrated at 25°C and 50% RH for 72 h. Then they were carefully placed and sealed using grease oil on the top of the glass cells ( $7.065 \times 10^{-4} \text{ m}^2$  in the internal surface area,  $19.625 \times 10^{-4} \text{ m}^2$  in the edge surface area, and 3.5 cm depth), which contained 8 ml saturated NaCl (74% RH). To prevent the leakage of moisture through the seals, in addition to using grease oil, circle rubber rings were put on the films as well as on the edges of the cells and tightly gripped by 4 metal clamps. The glass cells were put in a desiccator containing 800 gr silicagel at 25°C and 50% RH. The

cells were weighed every 5 h for 72 h. WVP was calculated as follows:

$$WVP = \frac{\Delta m \times X}{A \times \Delta t \times \Delta p} \quad (\text{Eq. 3})$$

Where, WVP is water vapor permeability (gr/m.hr.Kpa),  $\Delta m$  is total weight loss of the cells (gr),  $X$  is the thickness of the films (m),  $A$  is internal or exposed area of the film ( $\text{m}^2$ ),  $\Delta t$  is time of vapor penetration (hr), and  $\Delta p$  is pressure gradient ( $\Delta p = 2.368 \text{ Kpa}$  was calculated using a psychrometric chart from Universal Industrial Gases, Inc, Pennsylvania, USA).

**Color evaluations:** L\*, a\*, and b\* (mode of CIE) parameters of the nanocomposite films were measured in a tristimulus colorimeter (ColorFlex EZ, Bench top Spectrophotometers, USA). Five replicates were performed for each sample (30).

**Yellowness index (YI):** YI of the films was measured according to the ASTM standard E313-15 (33). Eq.4 was used for YI calculation:

$$YI = \frac{(C_x \cdot X - C_z \cdot Z)}{Y} \times 100 \quad (\text{Eq.4})$$

Where, XYZ are tristimulus factors, measured by a tristimulus colorimeter (ColorFlex EZ, Bench-top Spectrophotometers, USA), and  $C_x$  and  $C_z$  are constants obtained from the ASTM standard E313-15.

**Thickness:** Using a micrometer (Mitutoyo, Model0052526, Japan), the thickness of the nanocomposite films was measured. Five locations of the films were evaluated, and the average value was used for each sample.

**Statistical design:** The nanocomposite films were produced in a completely randomized design (CRD). The treatments were: 0 min of sonication time as control (PVA 0), 10 min (PVA 10), 20 min (PVA 20), 30 min (PVA 30), and 40 min (PVA 40). Design Expert ver.7.0 was used for optimization. Using numerical optimization, first goals for each response were set ten the software generated optimal conditions. Data were analyzed mainly in the SPSS software (ver. 20). Other statistical softwares such as MSTATC were also used. Multiple range Duncan's test was preformed for mean comparisons ( $\alpha=0.05$ ). All experiments and measurements were done with at least three replicates.

## Results

**MMT characterization:** MMT characteristics (Company datasheet, ZetaSizer results, and XRD results) are presented in Table 1. The XRD evaluation showed a peak in 8.7 2 $\theta$ , revealing 1.178 nm d-spacing between the silicate layers, which was near the reported d-spacing from the company.

**Mechanical properties:** Different ultrasound times had insignificant effect on elongation and Young's modulus of PVA nanocomposite films ( $p>0.05$ ), while they had significant effect on tensile strength of the films ( $P<0.01$ ). In comparison to the films without sonication, there was 22.28% enhancement in tensile strength due to applying 20 min of sonication time. Tensile strengths of the films are depicted in Fig.3. Young's modulus and elongation at break are reported in Table 2.

**WVP:** The effect of sonication time on the WVP of PVA films was not significant ( $p<0.05$ ). The obtained WVP data verifies that the time of sonication did not affect the WVP of PVA films. The results are reported in Table 3.

**Table 1.** MMT characteristics

Southern Clay Company data sheet (Cloisite Na <sup>+</sup> )					Zetasizer (0.4% Suspension)			XRD
d Spacing	MMT Thickness	Particle Size	Specific Weight	Bulk Density	Zeta Potential	Particle Size Average	Polydispersity Index (PDI)	d Spacing
1.17 nm	lower than 50nm	Lower than 2 $\mu$ m	2.86 g/ml	568 g/L	-30.4	195 nm	0.264	1.178 nm

**Table 2.** Elongation and Young's Modulus at different times of sonication

Time of Sonication (min)	Young's Modulus (MPa.)	Elongation (%)
0	2.3 $\pm$ 0.28 <sup>a</sup>	132.62 $\pm$ 5.25 <sup>a</sup>
10	2.5 $\pm$ 0.25 <sup>a</sup>	133.63 $\pm$ 5.5 <sup>a</sup>
20	2.15 $\pm$ 0.17 <sup>a</sup>	141.07 $\pm$ 3.04 <sup>a</sup>
30	2.35 $\pm$ 0.19 <sup>a</sup>	139.5 $\pm$ 4.12 <sup>a</sup>
40	2.32 $\pm$ 0.2 <sup>a</sup>	130.93 $\pm$ 5.9 <sup>a</sup>

\* Different letters show significant difference ( $p<0.05$ )

**Table 3.** WVP at different sonication times

Sonication times (min)	0	10	20	30	40
WVP (gr $\cdot$ m $^{-1}$ hr $^{-1}$ kpa $^{-1}$ $\cdot$ 10 $^{-3}$ )	0.376	0.369	0.344	0.339	0.345

**Table 4.** Optimization conditions and selected sample

Name	Goal	Lower Limit	Upper Limit	Importance	Selected Sample with 68.2 % Desirability
Ultrasound time	is in range	0	40	3	20
Tensil Stress	maximize	34.3	55.7	3	51.6
Elongation	is in range	103	169	3	157
wvp	minimize	0.258	0.453	5	0.33

**X-ray diffraction:** Increasing the ultrasound time caused enhancement of d-space between the MMT layers in nanocomposites. Table 5 and Fig. 4 show the changing trend of MMT d-space and the related XRD peaks in PVA nanocomposite films.

**FTIR Spectroscopy:** As shown in Table 6 and Figures 5 and 6, the ultrasound treatments had significant and wide effects on PVA nanocomposite films.

**Table 5.** d-space and peak angles of PVA films at different sonication times

Samples (min)	MMT	PVA20	PVA30	PVA40
d-Space (nm)	1.178	4.014	4.42	5.01
Peak Angles (2θ)	8.7	2.55	2.32	2.04

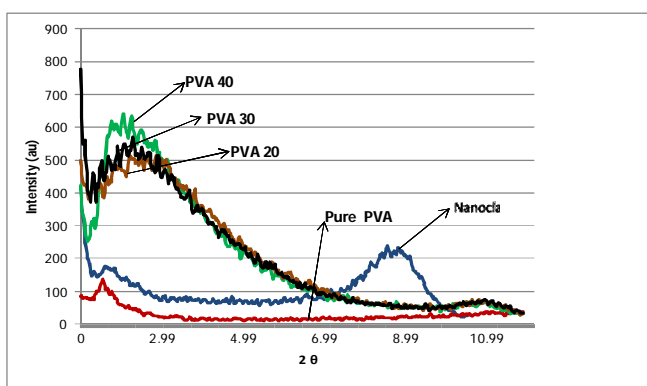


**Figure 4.** X-ray diffraction of PVA nanocomposites at different times of sonication

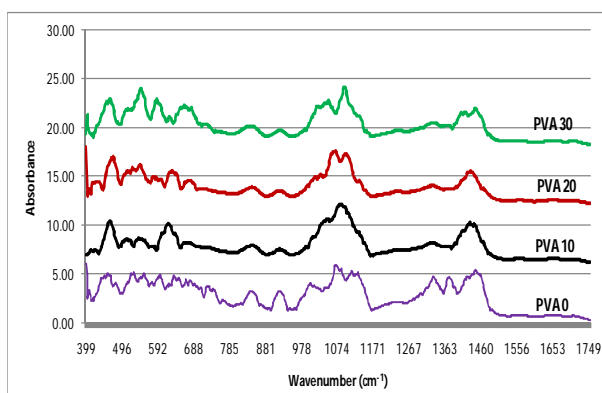


**Figure 5.** PVA FTIR spectra for low wave numbers

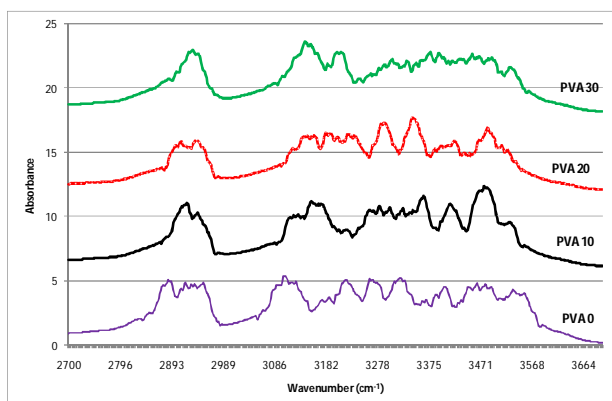


**Figure 6.** PVA FTIR spectra for low wave numbers

**Table 6.** Infrared spectra absorption data of PVA nanocomposite films at different times of sonication

Range	Low wave number range				High wave number range			
	PVA 0	PVA 10	PVA 20	PVA 30	PVA 0	PVA 10	PVA 20	PVA 30
Wave Numbers	454	464	469	460	2884	O	O	O
	528	O	539	546	2946	2915	2908	O
	593	O	589	593			2939N	2932
		509N	O	O	3110	O	O	O
		547N	O	O		3124N	O	O
	640	621	638	O		3165N	3150	3150
	680	675	677	668			3193N	O
	736	O	O	O				3206N
	844	845	846	841	3221	3274	3231	O
	920	921	920	921			3291N	O
	1009	O	O	O		3312N	O	3307
	1077	1086	1067	1048	3272	O	O	O
			1098N	1095	3321	O	O	O
	1121	O	O	O		3361N	3348	3387
	1236	1239	1239	1240	3401	3417	3415	3460
	1334	1330	1331	1332	3479	3480	3484	3485
	1378	O	O	O	3541	3524	O	3529
				1418N				
	1449	1437	1435	1449				
		1566N	1566	1565				
	1655	1656	1655	1656				

O: Omitted Peaks; N: New Peaks

**Opacity appearance:** Opacity is one of the most important features of the films, especially for food packaging. Ultrasound time had significant effect on the opacity of PVA nanocomposite films ( $p<0.05$ ). As you can see in Figure 7, sonication for 20 min had the lowest opacity (0.0006) in the PVA films.

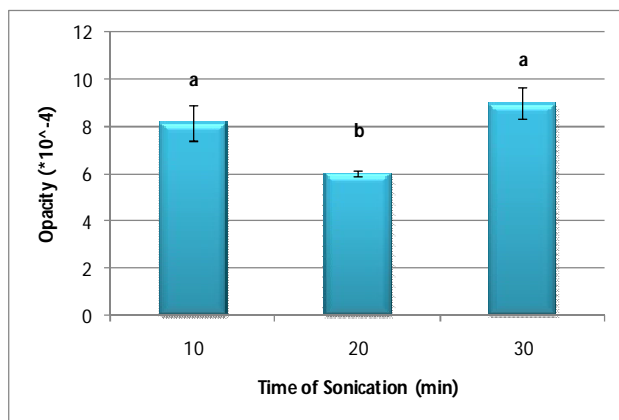


**Figure 7.** The effect of ultrasound time on the opacity of PVA nanocomposite films

**Color and YI:** Statistical analysis showed that time of sonication did not have any significant effect on  $L^*$ ,  $a^*$ , and YI of the PVA films, while it just affected significantly  $b^*$  ( $p<0.05$ ) (Fig. 8).

**Thickness:** The average thickness of the PVA films was 61.07 micron. It was not significantly changed in the samples with different times of sonication.

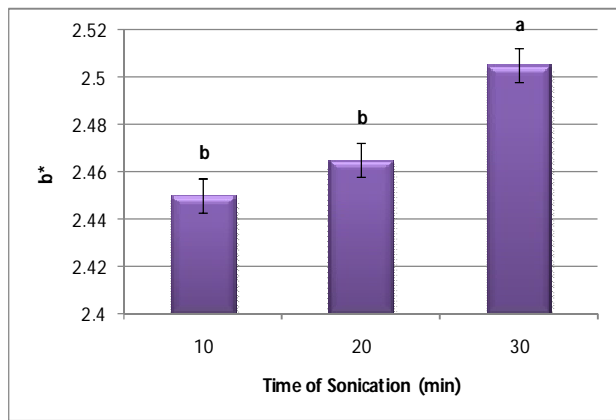


**Figure 8.** The effect of ultrasound time on  $b^*$  factor of PVA films

## Discussion

**MMT characterization:** Zetasizer evaluation demonstrated that zeta potential (ZP), particle size average (PSA), and polydispersity index (PDI) of the MMT suspension (0.4% w/v) were -30.4, 195 nm, and 0.264, respectively.

As reported in Table 1, PSA of MMT suspension was around 195 nm. Because 97.7% of the particles had similar size (260.9 nm), the suspension had high homogeneity. PSA from Zetasizer was nearly 10 times smaller than the value reported by company, which was because of soaking, stirring, and sonication of the treatments in the preparation of MMT (Fig. 1). So, these treatments surely decreased the size of the MMT particles. In compatible with this research, Alshabate et al. (2013) reported that Na-MMT suspension had a wide particle size distribution (three peaks), and around 88.2% of particles had 748.5 nm sizes, which is really more than the size of MMT suspension in the present study (3).

PDI is a dimensionless term for showing the band of size distribution, which usually ranges from 0.05 to 0.7 and, out of this range, especially more than 0.7, indicates that the sample is not probably suitable for evaluation by dynamic light scattering (DLS) technique in Zetasizer. PDI of the Na-MMT suspension in this study was 0.264 (Table 1), which was suitable and in the range (3, 34). ZP is a term that expresses the potential difference between the medium of suspension and the stationary layer of the fluid, which is attached to the dispersed particles. ZP of Na-MMT was -30.4 mv, indicating the moderate stability of the nano-particles (35).

**Mechanical properties:** As illustrated in Fig. 3, increasing the time of sonication up to 20 min caused enhancement of tensile strength. Then it was decreased at 30 min but not significantly at 40 min. Maximum tensile strength was 50.859 and 49.531 MPa at 10 and 20 min of sonication time, respectively (Fig. 3).

If sonication time and intensity increase more, the polymer and its chemical bonds would be probably decomposed; this will adversely affect its mechanical properties, like what has been seen at 20 and 30 min of sonication time. Several researchers have evaluated the effect of ultrasound radiation on different film properties and observed that tensile strength is improved, while different results are obtained about elongation (16, 17, 28, 36). As shown in Table 2, elongation increases up to 20 min of sonication and then decreases. The maximum elongation (141.07%) and tensile strength (50 MPa.) are related to 20 min of sonication; also the minimum Young's modulus (2.15 MPa.) was also corresponded to 20 min sonication (Table 2). Wang et al. (2014) and Cheng et al. (2010)

announced that increasing the time of sonication increased tensile strength up to a certain time, and decreased elongation. In the present study, this trend was expected but we observed that both tensile strength and elongation increased. Other papers have not used glycerol or other plasticizers. The hydroxyl groups of glycerol can attach to PVA by creating new H-bonds, and as a result, elongation will increase. The effect and role of glycerol might be a reason for obtaining the unexpected trends in this study, however, further experiments are needed to prove it. Lui et al. (2004) announced that both tensile strength and elongation of peanut protein films decreased by increasing the time of sonication. It shows that the effects of sonication time could be different depending to the material and formulation.

Mondal et al. (2013) announced that the tensile strength and elongation of PVA with 8% Na-MMT was 54.95 MPa and 160%, respectively. The reported values were near to those of the present research (29). The same results were also reported about the mechanical properties of PVA nanocomposites by Lui et al. (2014) (37). Chang et al. (2003) reported lower and higher elongation (9%) and tensile strength (160 MPa.), respectively (38). The reason of these differences could be related to PVA characteristics, especially the degree of polymerization and formulation of nanocomposites, which can extensively affect mechanical properties of the films.

If the solvent is water, usually active H and OH radicals and hydrogen peroxide will be generated. Several chemical reactions occurred between these active radicals and substances in the medium, like PVA, MMT, and glycerol in the present study. Finally, more chemical bonds (e.g. H and covalent bonds) were generated. Furthermore, sonication causes the exit of air bubble from the solution, which in turn results in more compact films with higher strength and resistance toward elongation (16). All of these mechanisms could be the reasons for improving the tensile strength at higher sonication times in PVA nanocomposites.

**WVP:** The minimum WVP in PVA films corresponded to 30 min sonication ( $0.33 \times 10^{-3}$  gr/m.hr.kpa). The data showed that 30 min of sonication time could decrease just 10.37% of WVP in comparison to the control film. In comparison to other papers, this depletion is low (16, 20). Mondal et al. (2013) reported the WVP of Na-MMT-PVA

nanocomposite films without glycerol as around  $0.03 \times 10^{-2}$  gr/m.hr, which is lower than the obtained value in the present research. As previously described, using glycerol in this research might be the reason of obtaining lower WVP.

**X-ray diffraction:** Fig.4 shows the X-ray diffraction (XRD) graph of PVA nanocomposite films. At first glance at XRD graph, we can find that the nanocomposites had intercalated structure, as the peak angle of pure MMT decreased from 8.7 to nearly 2 (Table 5) (26). It shows that increasing the time of sonication increased d-space between the MMT layers, and more incorporation of PVA/glycerol between the MMT layers occurred (8, 13).

Intensity/height of the XRD peaks shows the dispersity of MMT layers in the polymers. The lower intensity of the peaks had more scattering of MMT (8). The height of PVA XRD peaks was not noticeably different (Fig. 4), which shows that time of sonication did not have significant effect on the dispersion of MMT in PVA films. As the viscosity of PVA solution was not so high, probably magnet stirring was sufficient for dispersing MMT in PVA solution.

**Appearance of nanocomposites:** Changing opacity in PVA films did not show any logical trend (Fig. 7). As indicated in Fig. 7, 20 min time of ultrasound had the lowest opacity in comparison to 10 and 30 min. It shows that more air bubbles have been eliminated from the polymer solution at 20 min sonication, and some of the polymer's bonds have break down; therefore, the resulting film has got more transparent (16). In contrast to our expectation, opacity increased at 30 min sonication time, may be due to the formation of new chemical bonds at 30 min sonication time.

Figure 8 shows the trend of changing  $b^*$  factor by increasing the time of sonication but the reason is not really obvious. We can just explain that increasing the time of sonication could increase the compactness of the films, so transmittance decreased, and as a result,  $b^*$  (Yellow Color) increased. However, this result is not in accordance to the opacity of 30 min sonication time. There are no values and evidences in papers to describe the reasons of obtaining these results, and further researches are needed to clarify the reasons.

**FTIR Spectroscopy:** Ultrasound treatments caused disappearance of some peaks, and appearance of new ones. Most of the peaks shift positively, and got

sharper with higher intensity. It shows the incorporation of polymer/glycerol into the intergallery spacing of MMT layers and formation of new chemical bonds with MMT layers (3, 20, 39, 40). However, there are not outstanding differences, especially in low wave numbers, between the times of sonication (10, 20, and 30 min). In conclusion, the nanocomposite films should be optimized in terms of sonication to get the best quality. In comparison to methyl cellulose FTIR spectra, in another research by the authors, ultrasound had lower effects on PVA. The reason can be related to low molecular weight and viscosity of PVA in comparison to methyl cellulose. Therefore, the kind of polymer can play a key role in optimization of the time of sonication.

**Conclusion:** Sonication time remarkably affected the properties of the PVA nanocomposite films. Sonication time can emerge new bonds between polymers and nanomaterials, increase their intensity, and cause more dispersion of nanomaterial in polymer; as a result, properties of the films will be changed widely. Increasing the time of sonication could significantly change tensile strength, opacity, and  $b^*$  factor of PVA nanocomposites, while  $L^*$ , YI, and WVP did not change significantly. XRD and FTIR verified the effects of sonication time on the films properties. The results of this paper proves the importance and effects of time of sonication on film's traits. By optimizing and selecting appropriate time, the best quality can be achieved.

### Acknowledgement

We gratefully appreciate their kind cooperation. Also, we sincerely acknowledge the technicians of Food and Central Labs in Agricultural Faculty of TMU.

### Financial disclosure

The authors declare no financial interest.

### Funding/Support

This research was done with the financial support by the Tarbiat Modares university, as a part of a PhD dissertation.

### References

1. Alves V, Costa N, Hilliou L, Larotonda F, Gonçalves M, Sereno A, et al. Design of biodegradable composite films for food packaging. *Desalination*. 2006;199(1-3):331-3.
2. Avella M, De Vlieger JJ, Errico ME, Fischer S, Vacca P, Volpe MG. Biodegradable starch/clay nanocomposite films for food packaging applications. *Food Chem*. 2005;93(3):467-74.
3. Alshabanat M, Al-Arrash A, Mekhamer W. Polystyrene/montmorillonite nanocomposites: Study of the morphology and effects of sonication time on thermal stability. *J. Nanomate*. 2013;2013:9-.
4. Elbokl TA, Detellier C. Aluminosilicate nanohybrid materials. Intercalation of polystyrene in kaolinite. *J. Phys. Chem. Solids*. 2006;67(5-6):950-5.
5. Elbokl TA, Detellier C. Kaolinite-poly(methacrylamide) intercalated nanocomposite via in situ polymerization. *Can. J. Chem*. 2009;87(1 SPEC. ISS.): 272-9.
6. Rao Y. Gelatin-clay nanocomposites of improved properties. *Polymer*. 2007;48(18):5369-75.
7. Martucci JF, Vázquez A, Ruseckaite RA. Nanocomposites based on gelatin and montmorillonite: Morphological and thermal studies. *J. Therm. Anal. Calorim*. 2007;89(1):117-22.
8. Tunç S, Duman O. Preparation and characterization of biodegradable methyl cellulose/montmorillonite nanocomposite films. *Appl. Clay Sci*. 2010;48(3):414-24.
9. Theng BKG. The Chemistry of Clay-Organic Reactions. 29 King Street, London, WC2E 8JH: Adam Hilger Ltd., Rank Precision Industries.; 1974. 343pp. p.
10. Wang K, Chen L, Kotaki M, He C. Preparation, microstructure and thermal mechanical properties of epoxy/crude clay nanocomposites. *Composites Part A*. 2007;38(1):192-7.
11. Abd Alla SG, Nizam El-Din HM, El-Naggar AWM. Electron beam synthesis and characterization of poly(vinyl alcohol)/montmorillonite nanocomposites. *J. Appl. Polym. Sci*. 2006;102(2):1129-38.
12. Paul DR, Robeson LM. Polymer nanotechnology: Nanocomposites. *Polymer*. 2008;49(15):3187-204.
13. Morgan AB, Harris JD. Exfoliated polystyrene-clay nanocomposites synthesized by solvent blending with sonication. *Polymer*. 2004;45: 8695-703.
14. Adinoyi MJ, Merah N, Gasem Z, Al-Aqeeli N. Effect of sonication time and clay loading on nanoclay dispersion and thermal property of epoxy-clay nanocomposite. 8th International Conference on Composite Science and Technology, ICCST8; Kuala Lumpur2011b. p. 490-5.
15. Adinoyi MJ, Merah N, Gasem Z, Aqeeli N. Variation of mechanical properties of epoxy-clay nanocomposite with sonication time and clay loading. 8th International Conference on Composite Science and Technology, ICCST8; Kuala Lumpur2011a. p. 496-501.
16. Cheng W, Chen J, Liu D, Ye X, Ke F. Impact of ultrasonic treatment on properties of starch film-forming dispersion and the resulting films. *Carbohydr. Polym*. 2010;81(3):707-11.
17. Wang Z, Zhang N, Wang HY, Sui SY, Sun XX, Ma ZS. The effects of ultrasonic/microwave assisted treatment on the properties of soy protein isolate/titanium dioxide

films. *LWT - Food Science and Technology*. 2014;57(2):548-55.

18. Kentish S, Wooster TJ, Ashokkumar M, Balachandran S, Mawson R, Simons L. The use of ultrasonics for nanoemulsion preparation. *Innov. Food Sci. Emerg. Technol.* 2008;9(2):170-5.

19. Wang Z, Sun XX, Lian ZX, Wang XX, Zhou J, Ma ZS. The effects of ultrasonic/microwave assisted treatment on the properties of soy protein isolate/microcrystalline wheat-bran cellulose film. *J. Food Eng.* 2013;114(2):183-91.

20. Wang Z, Zhou J, Wang XX, Zhang N, Sun XX, Ma ZS. The effects of ultrasonic/microwave assisted treatment on the water vapor barrier properties of soybean protein isolate-based oleic acid/stearic acid blend edible films. *Food Hydrocoll.* 2014;35:51-8.

21. Zhong T, Lian Z, Wang Z, Niu Y, Ma Z. Influence of the Microwave and Ultrasonic synergistic effect on properties of methylcellulose/stearic acids films. 2nd Environment-Enhancing Energy and Biochemicals Conference, EC2SH 2012. Shanghai2013. p. 51-4.

22. Bochek AM, Zabivalova NM, Lavrent'ev VK, Abalov IV, Gofman IV. Properties of mixed aqueous solutions of methyl cellulose with polyethylene oxide and of composite films prepared from them. *Russ. J. Appl. Chem.* 2011;84(9):1575-81.

23. Dobrovolskaya IP, Yudin VE, Drozdova NF, Smirnova VE, Gofman IV, Popova EN, et al. Structure and characteristics of film composites based on methyl cellulose, poviargol, and montmorillonite. *Polymer Science - Series A*. 2011;53(2):166-71.

24. DeMerlis CC, Schoneker DR. Review of the oral toxicity of polyvinyl alcohol (PVA). *Food Chem. Toxicol.* 2003;41(3):319-26.

25. Tang X, Alavi S. Recent advances in starch, polyvinyl alcohol based polymer blends, nanocomposites and their biodegradability. *Carbohydr. Polym.* 2011;85(1):7-16.

26. Strawhecker KE, Manias E. Structure and Properties of Poly(vinylalcohol)/Na+Montmorillonite a nocomposites. *Chem Mater.* 2000;12:2943-9.

27. ASTM. Standard Test Method for Tensile Properties of Thin Plastic Sheeting. Designation: D882-12. ASTM International, West Conshohocken, PA, [www.astm.org2012](http://www.astm.org2012).

28. Liu CC, Tellez-Garay AM, Castell-Perez ME. Physical and mechanical properties of peanut protein films. *LWT - Food Science and Technology*. 2004;37(7):731-8.

29. Mondal D, Mollick MMR, Bhowmick B, Maity D, Bain MK, Rana D, et al. Effect of poly(vinyl pyrrolidone) on the morphology and physical properties of poly(vinyl alcohol)/sodium montmorillonite nanocomposite films. *Progress in Natural Science: Materials International*. 2013;23(6):579-87.

30. Giménez B, Gómez-Estaca J, Alemán A, Gómez-Guillén MC, Montero MP. Physico-chemical and film forming properties of giant squid (*Dosidicus gigas*) gelatin. *Food Hydrocoll.* 2009;23(3):585-92.

31. Gómez-Estaca J, Montero P, Fernández-Martín F, Alemán A, Gómez-Guillén MC. Physical and chemical properties of tuna-skin and bovine-hide gelatin films with added aqueous oregano and rosemary extracts. *Food Hydrocoll.* 2009;23(5):1334-41.

32. ASTM. Standard Test Methods for Water Vapor Transmission of Materials. Designation: E96/E96M-14. ASTM International, West Conshohocken, PA, 2014, [www.astm.org2014](http://www.astm.org2014).

33. ASTM. Standard Practice for Calculating Yellowness and Whiteness Indices from Instrumentally Measured Color Coordinates. Designation: ASTM E313-15. ASTM International, West Conshohocken, PA, [www.astm.org2015](http://www.astm.org2015).

34. Bohren CF, Huffman DR. Absorption and scattering of light by small particles: John Wiley & Sons; 2008.

35. Honary S, Zahir F. Effect of zeta potential on the properties of nano-drug delivery systems - A review (Part 1). *Trop. J. Pharm. Res.* 2013;12(2):255-64.

36. Marcuzzo E, Peressini D, Debeaufort F, Sensidoni A. Effect of ultrasound treatment on properties of gluten-based film. *Innov. Food Sci. Emerg. Technol.* 2010;11(3):451-7.

37. Liu G, Song Y, Wang J, Zhuang H, Ma L, Li C, et al. Effects of nanoclay type on the physical and antimicrobial properties of PVOH-based nanocomposite films. *LWT - Food Science and Technology*. 2014;57(2):562-8.

38. Chang J-H, Jang T-G, Ihn KJ, Lee W-K, Sur GS. Poly(vinyl alcohol) nanocomposites with different clays: Pristine clays and organoclays. *J. Appl. Polym. Sci.* 2003;90(12):3208-14.

39. Madejová J. FTIR techniques in clay mineral studies. *Vib. Spectrosc.* 2003;31(1):1-10.

40. Tzavalas S, Gregoriou VG. Infrared spectroscopy as a tool to monitor the extent of intercalation and exfoliation in polymer clay nanocomposites. *Vib. Spectrosc.* 2009;51(1):39-43.